

0338-1 **EFFECTIVENESS AND ECONOMY OF HYDROGEN PRODUCTION BY  
NATURAL GAS DECOMPOSITION IN THE THERMAL PLASMA**

**Dejan Cvetinović<sup>1</sup>, Aleksandar Erić<sup>1</sup>, Nikola Živković<sup>1</sup>,  
Jovana Anđelković<sup>1</sup>, Predrag Škobalj<sup>1</sup>, Gleb Belov<sup>2</sup>**

*<sup>1</sup>«Vinča» Institute of Nuclear Sciences – National Institute of the Republic of Serbia,  
University of Belgrade, Laboratory for Thermal Engineering and Energy,  
Mike Petrovica Alasa 12-14, 11351 Vinca, Belgrade, Serbia, deki@vin.bg.ac.rs*

*<sup>2</sup>Joint Institute for High Temperatures, Russian Academy of Sciences, Lomonosov Moscow State  
University, Izhorskaya ul. 13, str. 2, Moscow, 125412 Russian Federation, gbelov@yandex.ru*

Abstract: Hydrogen produced by the thermal decomposition of natural gas in a low-temperature plasma reactor is the subject of this study. The main advantage of plasma pyrolysis of natural gas is that a high yield of hydrogen can be obtained without the emission of carbon monoxide or carbon dioxide since the main products of the process are carbon in the solid state and hydrogen. The use of plasma allows the decomposition of natural gas without the use of catalysts, which is one of the main problems of current technologies for hydrogen production from this feedstock. In this paper, an analysis of the process is presented using a thermodynamic equilibrium model based on the minimum of the Gibbs function in the temperature range of 500-2500 K. Undesirable components in the system such as carbon dioxide, hydrogen cyanide and nitrogen compounds such as ammonia and nitric oxide are evaluated. The analysis showed the useful energy of the system per kilogram of feedstock and the efficiency of the high-temperature plasma decomposition process in terms of hydrogen produced. The results of the numerical analysis showed an optimal temperature for the process evaluation of about 1200 K, at which an efficiency of about 50 % is achieved.

**Keywords:** hydrogen production, natural gas, thermal plasma reactor, pyrolysis, thermodynamic equilibrium

**NOMENCLATURE:**

$a_{ij}$	[-]	number of atoms of the $j^{\text{th}}$ element in the $i^{\text{th}}$ chemical species
$A_j$	[-]	total number of atoms of the $j^{\text{th}}$ element in the system
$A_{r,i}$	[/]	relative atomic mass of the $i^{\text{th}}$ element
$f_a$	[/]	treated and working medium mass flow ratio
$G$	[J]	Gibbs free energy
$g_i$	[kg/kg]	mass fraction of the $i^{\text{th}}$ chemical species in the system

0338,2		
$g_i$	[J/mol]	specific standard Gibbs free energy
$H$	[J]	enthalpy
$h_i^0$	[J/mol]	specific enthalpy of the $i^{\text{th}}$ system component at standard conditions
$h_{f,0}$	[kJ/kg]	specific physical enthalpy of the treated medium at standard conditions
$h_{HV,i}$	[J/mol]	molar heat value of the $i^{\text{th}}$ fuel component of the system
$h_s$	[kJ/kg]	specific enthalpy of the system
$h_{wm,T_1}$	[kJ/kg]	specific enthalpy of the system at the required temperature
$h_{wm,0}$	[kJ/kg]	specific physical enthalpy of the working medium at standard temperature
$M_i$	[g/mol]	molar mass of the $i^{\text{th}}$ chemical species
$\dot{m}_{wm}$	[kg/s]	mass flow of the working medium
$\dot{m}_f$	[kg/s]	mass flow of the treated medium
$n_N$	[mol]	ukupni broj molova sistema
$n_i$	[mol]	number of moles
$P_{sg}$	[W]	power of the fuel components of the system
$R$	[J/(molK)]	universal molar gas constant
$S$	[J/K]	entropy
$s_i^0$	[J/(molK)]	specific entropy of the $i^{\text{th}}$ system component at standard conditions
$T$	[K]	temperature
$u$	[g]	atomic mass unit
$x_i$	[mol/mol]	molar fraction of the $i^{\text{th}}$ chemical species in the system
$\Delta_f h_f^0$	[kJ/kg]	specific enthalpy of formation of the treated medium at standard conditions
$\Delta_f h_{wm}^0$	[kJ/kg]	specific enthalpy of formation of the working medium at standard conditions
$\varepsilon_E$	[W <sub>e</sub> /W <sub>sg</sub> ]	required electrical power to the power of the fuel components ratio
$\eta_{wm}$	[/]	electrical energy to plasma energy conversion ratio
$\lambda_k$	[-]	Lagrange multiplier
$\mu_i$	[J/mol]	chemical potential

## 1. INTRODUCTION

With the introduction of the Renewable Energy Directive (2009/28/ EC) in 2009, the share of renewable energy has increased annually and will reach 22 % in 2020. The Renewable Energy Directive has been revised several times to provide a path to climate neutrality by 2050. The previous target for the share of renewable energy in EU energy consumption by 2030 was 32 %. In July 2021, the target was increased to 40 %, while recently, in September 2022, it was raised again to 45 % [1]. Hydrogen has been identified as one of the main alternatives to achieve net zero greenhouse gas (GHG) emissions announced by governments in recent years. According to the work of Ajanović et al [2], hydrogen can be categorized as 'grey', 'blue', 'turquoise', 'green' and 'purple', which are shown in Fig. 1. In 2021, hydrogen demand reached 94 million metric tons (Mt), resulting in greenhouse gas emissions of 900 Mt CO<sub>2</sub> [3]. Hydrogen was used in refineries to remove impurities such as sulfur (40 Mt), in the industrial

sector to produce ammonia (34 Mt) and methanol (15 Mt), in the steel industry (5 Mt), in transportation for heavy road and rail vehicles (30 kt), while hydrogen demand in the building and energy sectors accounted for a negligible share. Most of the hydrogen demand in 2021 was met by 'grey' hydrogen, 62 % of which was produced from natural gas, 18 % from naphtha reforming in refineries, and 19 % from coal, so there were no environmental benefits from lower greenhouse gas emissions. At the same time, the production of 'blue' hydrogen was less than 1 million tons [3]. Nevertheless, 'blue' and 'turquoise' hydrogen will play an important role in the following energy transition, especially to reduce emissions from fossil fuels in the short term until sufficient energy can be produced from renewable sources or large-scale hydrogen transport is possible.

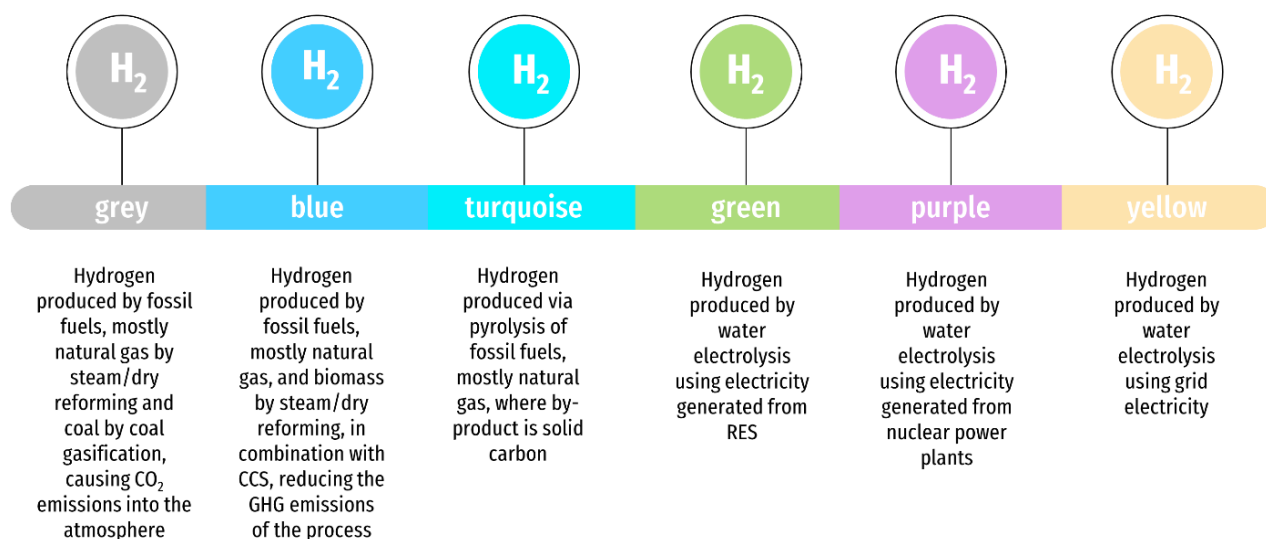
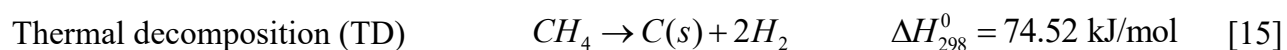
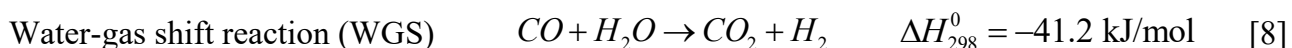
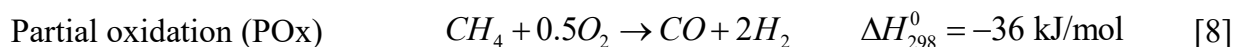
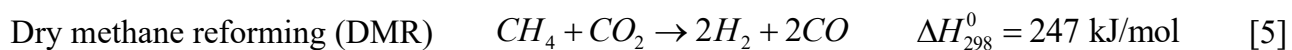
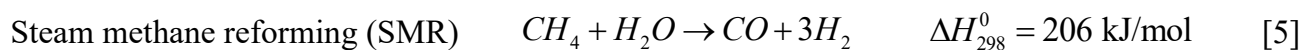


Fig. 1. The “colours” of hydrogen, adapted from [2]

The advantages and disadvantages of the most common hydrogen production technologies such as natural gas reforming, water electrolysis, and photobiological and thermochemical processes are presented in the work of Bepalko et al [4]. Hydrogen can be produced from natural gas by several processes: Steam Methane Reforming (SMR), Dry Methane Reforming (DMR), Partial Oxidation (POx) and Thermal Decomposition (TD). SMR uses methane from natural gas, which is reacted with steam under a pressure of 0.3-2.5 MPa in the presence of a nickel-based or alumina catalyst and converted to syngas, a mixture of hydrogen, carbon monoxide, and a few other components [5], [6]. The process is carried out at temperatures higher than 800 °C, which are often achieved by burning methane as the starting gas [7], [8]. In the case of DMR, methane reacts with carbon dioxide to produce syngas with an H<sub>2</sub>/CO-mole ratio close to 1. Both of the aforementioned processes are endothermic, i.e., they require a large amount of energy. POx, on the other hand, is an exothermic reaction with the advantage that the energy requirement for the reforming process is lower. The syngas produced by the aforementioned technologies is then converted into a hydrogen-rich mixture in a reactor, where high-purity hydrogen can be obtained by a water gas shift (WGS) reaction in which the carbon monoxide produced reacts with water vapour to produce more hydrogen. On the other hand, the WGS reaction can lead to excessive carbon dioxide generation in hydrogen-rich gas, as reported in the work of Shagdar et

0338-49]. Pressure swing adsorption (PSA) is used as the last step to remove mainly carbon dioxide, but also water, methane and carbon monoxide from hydrogen-rich gas [10] and to obtain high-purity hydrogen of 99 % [6]. Thermal decomposition of methane, also known as pyrolysis [11] or methane cracking [12], is a process that decomposes methane into carbon and hydrogen without producing carbon dioxide or carbon monoxide [13], which makes it a very attractive technology because it does not require a carbon capture, utilization, and storage (CCUS) system. The decomposition of methane starts at 500-600 °C, but to obtain a high yield of hydrogen, much higher temperatures should be used, especially if the process is carried out without a catalyst. It is worth mentioning that during the decomposition process, carbon produced as a by-product can play a catalytic role and increase the conversion of methane and hydrogen yield [14].



Hrabovsky et al [5] have highlighted the limitations of the above technologies related to the need to use catalysts to achieve high methane conversion rates. Park et al [8] and Iulianelli et al [16] also pointed out that studies on these processes pay great attention to the catalysts used in the process, their activity and stability, the effect of the type and amount of active metal on catalyst performance, and the identification of causes of deactivation such as sintering of metallic species and coke deposition. Fan et al [17] reported that it is difficult for the catalysts to exhibit high activity and long-term stability simultaneously, so most solid catalysts have a lifetime of fewer than 10 hours. Finding suitable catalyst candidates for the SRM process is a major technical challenge because the use of catalysts greatly affects the performance of the process. Among the most studied catalysts are materials such as Ni, Fe, Co, Al, Ru, Rh, Pd, Ir, and Pt [18]. Choi et al [7] added that the use of noble metals as catalysts is expensive and prone to impurities with species such as sulfur, and suggested using steam plasma reforming without a catalyst. The steam methane reforming can currently be considered a mature process, and commercial catalysts have an improved lifetime, even now days most of the problems belong to the coke deposition, which is avoided by using high water rates.

The use of plasma in methane conversion offers several advantages, such as the high quality of the synthesis gas produced, easy control of its composition, compatibility with a wide range of hydrocarbons (natural gas, heavy oils, and biofuels), compactness and fast reaction time since the

plasma is powered by electricity and the fact that no catalysts are needed and thus there is no risk of catalyst sensitivity and wear [5], [7], [19]. Due to the high temperatures and high ionization corresponding to plasma conditions, thermodynamically favorable chemical reactions can be accelerated and endothermic reforming processes can be energized without the use of a catalyst [20]. Different types of non-thermal and thermal plasmas have already been used for the conversion of methane to hydrogen. Among non-thermal plasmas are dielectric barrier discharges (DBD) [21], [22] and gliding arc discharges [23], [24], while among thermal plasmas are alternating current (AC) [25], Radiofrequency (RF) [26], microwave plasmas (MW) [7], [27]-[29] and also hybrid modifications such as direct current (DC) spark discharge plasma [30], AC gliding arc discharge [31], DC-RF [32], etc.

Hrabovsky et al [5] studied dry and steam methane reforming in thermal plasma and performed calculations on the equilibrium composition of the reaction products and energy balances. The observed temperature range was 400-6000 K, the pressure was 0.1 MPa, and the chemical species considered were: C<sub>2</sub>, C<sub>3</sub>, CO, CO<sub>2</sub>, C<sub>3</sub>O<sub>2</sub>, CH, CH<sub>2</sub>, CH<sub>3</sub>, CH<sub>4</sub>, HCO, H<sub>2</sub>CO, C<sub>2</sub>H, C<sub>2</sub>H<sub>2</sub>, C<sub>2</sub>H<sub>4</sub>, O<sub>2</sub>, O<sub>3</sub>, H<sub>2</sub>, OH, HO<sub>2</sub>, H<sub>2</sub>O, and H<sub>2</sub>O<sub>2</sub>. The equilibrium composition of the synthesis gas for methane steam reforming exhibited significantly higher yields of hydrogen and hydrogen in atomic form than dry steam reforming, where the carbon monoxide yield was higher than the hydrogen yield. The authors also performed experimental studies and reported that the minimum energy required to produce 1 kg of hydrogen was 79 MJ for steam reforming and 116 MJ for dry reforming, and corresponded to the energy expended for the process in the reactor volume rather than the total energy consumed, which includes torch efficiency and power loss in the reactor. Czyilkowski et al [28] presented experimental results of hydrogen production by atmospheric microwave plasma combined with steam reforming of methane. They observed the hydrogen production rate (how many grams of hydrogen are produced per 1 hour), the energy yield of hydrogen production (the ratio of the hydrogen production rate to the absorbed microwave power), the methane conversion efficiency, and the volume concentration of hydrogen in the exhaust gas. The results showed that the absorbed microwave power ranged from 3.5 to 4.5 kW, and the hydrogen production rate, methane conversion efficiency, and hydrogen concentration increased, while the energy yield decreased as the absorbed microwave power increased. The best results for hydrogen production rate and energy yield were 192 gH<sub>2</sub>/h and 42.9 gH<sub>2</sub>/kWh, respectively. Abanades et al [33] reported that in catalytic cracking, the temperatures are below 1000 °C, but the problem is catalyst deactivation due to coke formation.

The carbon black industry has struggled to keep pace with both tightening environmental regulations and the incumbent technology relying on thermal-oxidative decomposition of heavy aromatic oils. Monolith Corporation is a leader in this space, having successfully commercialized its methane pyrolysis process utilizing an electric plasma torch to thermally decompose natural gas into carbon black and hydrogen. The Monolith plasma-based technology is combustion free and has a substantially reduced environmental footprint relative to traditional carbon black manufacturing.

Monolith has a vision for its technology to play a key role in the pathway to net-zero through carbon-free hydrogen and clean carbon black [34].

Further research on methane cracking is needed because the most important prerequisite for the development of a reliable technology for hydrogen production that can be used on a large scale is to be able to operate in continuous mode, which has not yet been achieved. In this paper, the results of a numerical study of the thermal plasma decomposition process of natural gas for obtaining a high yield of hydrogen are presented. The equilibrium model is based on the minimum of the Gibbs function and was explained in our previous work [35, 36, 37] on cases of agricultural biomass and hazardous waste in steam or air plasma gasification. The objective of the study is to demonstrate the effectiveness of the proposed operating conditions on the efficiency of the process. The parameters of interest are the equilibrium composition of the system in the studied temperature range with special attention to the undesirable components such as carbon dioxide, hydrocyanic acid, and nitrogen compounds, and a ratio of useful and input power of the system.

## 2. MATERIALS AND METHODS

### 2.1. Thermodynamic equilibrium model

By modifying the Clausius, inequality for irreversible processes a process in a system at constant pressure and temperature is spontaneous if the total entropy change (system and environment) is greater than zero, and the enthalpy change is less than zero. The enthalpy possessed by a thermodynamic system can be used partially, which depends on the state of the environment, so it consists of a usable and an unusable part. The maximum possible energy that can be obtained at constant pressure from a system is essentially the maximum non-expansion work or Gibbs free energy, which can be determined as

$$G = H - TS \quad (1)$$

When it comes to a system consisting of  $i=1, N$  chemical species, the concept of chemical reactivity of each species is introduced, as a special state quantity. Looking back at the definition of Gibbs energy, as the maximum available energy of the system, it is concluded that chemical reactivity is nothing but a partial molar Gibbs function. Therefore, Eq. (1) can be written in the following form

$$G = \sum_{i=1}^N n_i \cdot \mu_i \quad (2)$$

At constant pressure, the activity of the  $i^{th}$  component of the system can be defined as follows

$$\mu_i = g_i^0 + RT \ln \left( \frac{n_i}{n_N} \right) \quad (3)$$

0338-7 Combining equations (2) and (3) gives the expression for the total Gibbs free energy

$$G = \sum_{i=1}^N n_i \cdot \left( g_i^0 + RT \ln \left( \frac{n_i}{n_N} \right) \right) \quad (4)$$

The expression for free Gibbs energy (4) contains the standard enthalpy of formation of the  $i^{\text{th}}$  chemical species. According to the condition of the spontaneity of the process in a system, the equilibrium composition will be reached in the case when the total Gibbs free energy reaches a minimum value [38, 39]. Therefore, to determine the equilibrium composition of the system, it is necessary to determine the coordinates of the minimum of equation (4) while respecting the boundary condition

$$\sum_{i=1}^N a_{ij} \cdot n_i = A_j \quad j = \overline{1, M} \quad (5)$$

where  $a_{ij}$  is the number of atoms of the  $j^{\text{th}}$  element in the  $i^{\text{th}}$  chemical species,  $A_j$  is the total number of atoms of the  $j^{\text{th}}$  element in the system. To determine the minimum of equation (4), it is most suitable to use the method of undetermined multipliers of the Lagrange function

$$L = \sum_{i=1}^N n_i \cdot \left( g_i^0 + RT \ln \left( \frac{n_i}{n_N} \right) \right) + \sum_{k=1}^K \lambda_k \cdot a_{ij} \cdot n_i - A_j \quad \lambda_k = \overline{1, K} \quad (6)$$

By differentiating equation (6) by all independent variables and equating the differential to zero, an equilibrium system is obtained that establishes a connection between the parameters of the system in equilibrium [40, 41].

$$g_i^0 + RT \ln \left( \frac{n_i}{n_N} \right) + \sum_{k=1}^K \lambda_k \cdot a_{ij} \geq 0 \quad (7)$$

$$n_N = \sum_{i=1}^N n_i \quad (8)$$

$$\sum_{i=1}^N a_{ij} \cdot n_i = A_j \quad j = \overline{1, M} \quad (9)$$

Expression (7) can also be written in the following form

$$n_i \geq n_N \cdot \exp \left( \left( -g_i^0 + \sum_{k=1}^K \lambda_k \cdot a_{ij} \right) / RT \right) \quad (10)$$

The inequality sign in equation (7) comes from the condition of achieving the minimum of the function  $L$  ( $\partial L \geq 0$ ), where if the corresponding chemical species exist in the system, the equality sign appears in equation (7). By replacing expression (10) in expressions (8) and (9) with the condition of the existence of a chemical species, a system of equations is obtained

$$n_N \sum_{i=1}^N a_{ij} \cdot \exp\left(\left(-g_i^0 + \sum_{k=1}^K \lambda_k \cdot a_{ij}\right) / RT\right) = A_j \quad (11)$$

and

$$n_N \left[ \exp\left(\left(-g_i^0 + \sum_{k=1}^K \lambda_k \cdot a_{ij}\right) / RT\right) - 1 \right] = 0 \quad (12)$$

The solution of the system of equations (11)-(12) is obtained by an iteration procedure, which results in the chemical composition of the system that is in thermodynamic equilibrium.

The value of the standard Gibbs free energy is determined based on equation (1) using available databases

$$g_i^0 = h_i^0 - T \cdot s_i^0 \quad (13)$$

The total enthalpy of the system,  $H_s$  at temperature  $T$ , is calculated by summing the specific enthalpies of all species.

$$H_s(T) = \sum_{i=1}^N n_i \cdot h_i(T) \quad (14)$$

The polynomial coefficients of the temperature dependence of the Gibbs free energies and the heat of formation (at the standard condition and temperature 0 K) of species, were taken from the literature [38, 39]. These data correspond to the data of JANAF.

## 2.2. Mass and energy balance

This research work discusses the process of thermal decomposition or pyrolysis of methane, the main component of natural gas, in a low-temperature plasma reactor to obtain a high yield of hydrogen. The composition and properties of the natural gas used in the model are given in Tab. 1.

Table 1. Natural gas composition and characteristics at the reactor inlet

Gas components				Lower heating value	Higher heating value	Density
CH <sub>4</sub>	C <sub>2</sub> H <sub>6</sub>	N <sub>2</sub>	CO <sub>2</sub>	LHV	HHV	$\rho_g$
%vol				kJ/m <sup>3</sup>	kWh/m <sup>3</sup>	kg/m <sup>3</sup>
95.96	2.16	0.72	0.28	34,798.00	11.31	0.71

It was assumed that the fuel (natural gas) enters the plasma reactor at a temperature of 25 °C (298.15 K), passes through an electric arc, and at the exit are obtained the components of the system that are in thermodynamic equilibrium at a certain (desired) temperature. As the fuel passes through the plasma reactor, it receives the energy of the electric arc, breaking the covalent bonds in the hydrocarbon molecules (CH<sub>4</sub> and C<sub>2</sub>H<sub>6</sub>) and producing carbon in the solid phase (graphite) and hydrogen (H<sub>2</sub>). Although dissociation of hydrogen occurs at higher temperatures, above 2000 K, it is not of interest in



this study because the dissociated hydrogen atoms reassemble very quickly into a stable hydrogen molecule as the system cools. Carbon in the solid state, which is a byproduct of the process, is usually in the form of graphite, i.e., soot, and is therefore considered an undesirable side effect in this study. Otherwise, high temperatures and the presence of a large amount of carbon in the reactor lend themselves to the production of other carbonaceous compounds, such as calcium carbide ( $\text{CaC}_2$ ), silicon carbide ( $\text{SiC}$ ), and many others.

After choosing the optimal temperature of the system, the required power of the plasmatron can be determined. The power is calculated based on the required enthalpy of the working fluid to achieve the desired system temperature. The required enthalpy of the working fluid can be calculated by establishing the energy balance of the system in the following form

$$\dot{m}_{wm} + \dot{m}_f \cdot h_s = \dot{m}_{wm} \cdot h_{wm,T_1} + \dot{m}_f \cdot h_{f,0} + \Delta_f h_f^0 \quad (15)$$

where  $\dot{m}_{wm}$ ,  $\text{kg}/s$  - the mass flow of the working medium,  $\dot{m}_f$ ,  $\text{kg}/s$  - the mass flow of the treated medium,  $h_s$ ,  $\text{kJ}/\text{kg}$  - the specific enthalpy of the system at the optimum temperature,  $h_{wm,T_1}$ ,  $\text{kJ}/\text{kg}$  - the required specific enthalpy of the working medium,  $h_{f,0}$ ,  $\text{kJ}/\text{kg}$  - the specific enthalpy of the treated medium at the reference temperature,  $\Delta_f h_f^0$ ,  $\text{kJ}/\text{kg}$  - the enthalpy of formation of the treated medium at the reference temperature. Based on equation (1), the required enthalpy of the working fluid can be expressed as follows

$$h_{wm,T_1} = \frac{\dot{m}_{wm} + \dot{m}_f \cdot h_s - \dot{m}_f \cdot h_{f,0} + \Delta_f h_f^0}{\dot{m}_{wm}} \quad (16)$$

In the ideal case, if all losses in the conversion of electrical energy to plasma energy of the working medium are neglected, the required power is equal to the product of the mass flow and the difference between the required enthalpy and the enthalpy at the reference temperature:

$$P_{wm} = \dot{m}_{wm} \cdot [h_{wm,T_1} - h_{wm,0} + \Delta_f h_{wm}^0] \quad (17)$$

where  $h_{wm,0}$  - is the physical enthalpy of the working medium at the reference temperature and  $\Delta_f h_{wm}^0$ ,  $\text{kJ}/\text{kg}$  - is the enthalpy of creation of the working fluid at the reference temperature.

A system at optimum temperature contains a considerable amount of energy, but only a portion of this energy can be utilised because the system must undergo a rapid cooling process to prevent the formation of unwanted compounds. The useful energy of the system is equal to the energy contained in the fuel components of the system at the reference temperature. At this temperature, if the physical enthalpy of the fuel components of the system is neglected relative to the enthalpy of formation, the useful energy of the system is equal to the product of the mass flow rate and the lower heating values of the combustible components.

$$P_{sg} = \dot{m}_{wm} + \dot{m}_f \cdot \sum_{i=1}^n x_i \cdot h_{HV,i} \quad (18)$$

where  $x_i$   $mol/kg_s$  - is the number of moles of the combustible components per kilogram of the system,  $h_{HV,i}$ ,  $kJ/mol$  - is the heat output of the fuel component of the system per one mole, and  $n$  is the number of combustible components of the system.

The ratio of these powers can be expressed in terms of the electrical power required to produce one unit of syngas power

$$\varepsilon_E = \frac{P_{wm}}{\eta_{wm} \cdot P_{sg}} \quad (19)$$

where  $\eta_{wm}$  / is the ratio of conversion of electrical energy into plasma energy of the working fluid.

### 3. RESULTS AND DISCUSSION

Figures 2-4 show the equilibrium composition of the system as a function of temperature determined by the presented methodology of pyrolysis of natural gas in a low-temperature plasma reactor.

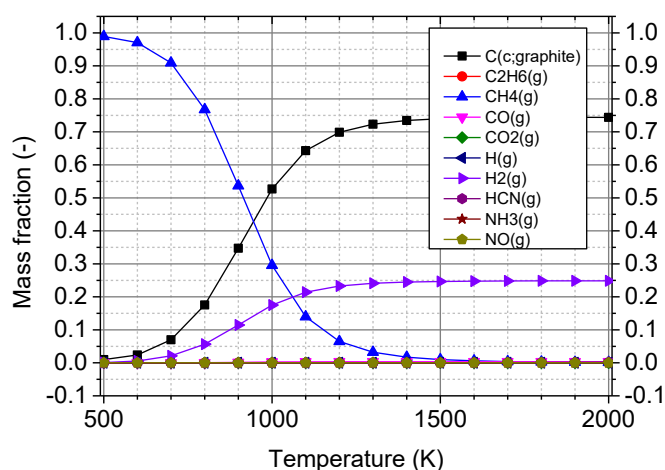


Fig. 2 Mass fractions of system components

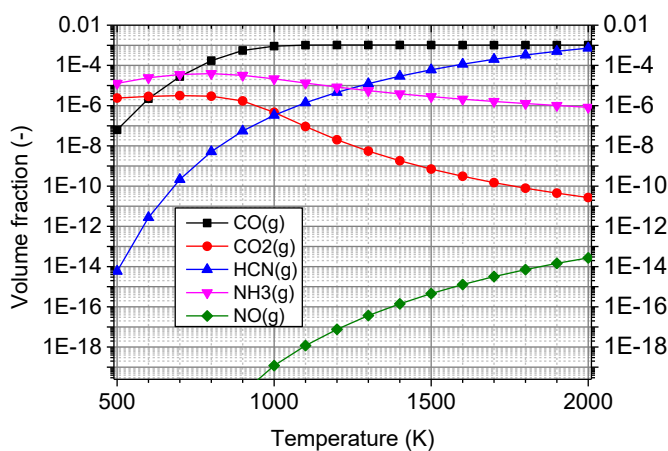


Fig. 4 Volume fraction of undesirable components

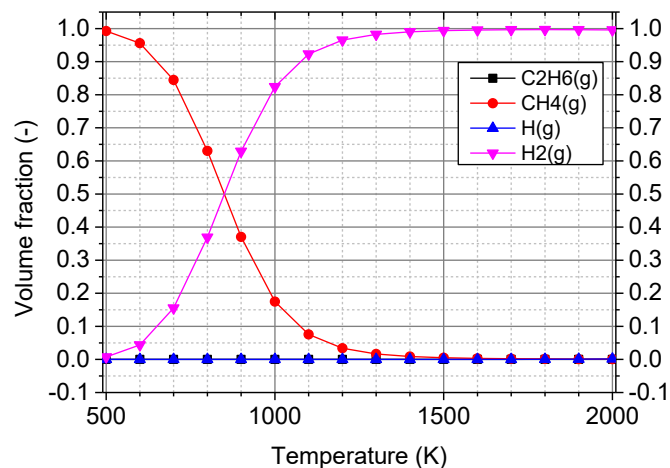


Fig. 3 Volume fraction of system components

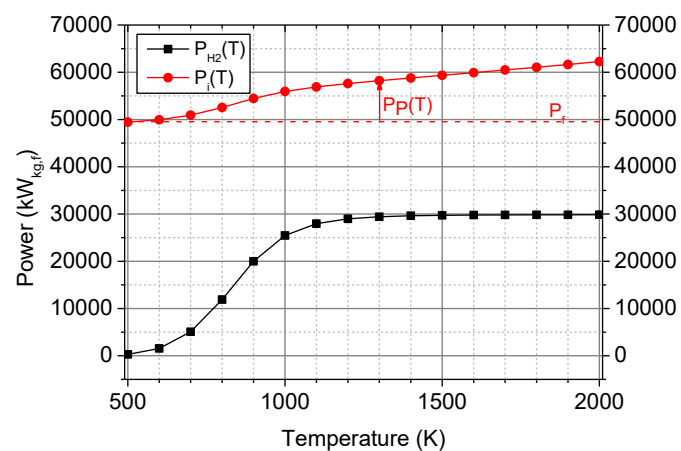


Fig. 5 Useful power and input power

Figures 1-2 clearly show that the proportion of combustible components, especially methane, decreases with increasing temperature, while the proportion of graphite and hydrogen in molecular form

0338-11 increases in proportion to its decrease. This process is practically completed at a temperature of 1500 K. Undesirable components of the system are shown in Fig. 3, where it is noticeable that with increasing temperature the proportion of hydrocyanic acid and nitrogen monoxide increases, while the proportion of ammonia and carbon dioxide decreases. The proportion of carbon monoxide increases sharply up to a temperature of 1000 K, after which its growth stops and the value does not change with a further increase in temperature. Considering that the proportions of nitrogen monoxide and hydrogen cyanide increase more than the proportions of ammonia and carbon dioxide decrease with increasing temperature, as well as the fact that the first two undesirable compounds are harmful, it can be concluded that, from this point of view, a lower temperature is more suitable.

The energy analysis, shown in Fig. 4, indicates that the useful energy of the system per kilogram of fuel increases with the increase of the process temperature, reaching a maximum value of about 1500 K, after which it remains constant with a further increase in temperature. This is to be expected considering that the maximum fuel conversion has taken place in the process, i.e., complete pyrolysis of natural gas has occurred and the maximum possible concentration of hydrogen has been reached. The input power per kilogram of fuel is composed of the power supplied by the fuel (natural gas) and the power of the plasma reactor. The power of the fuel is a constant value and is defined by the mass flow of the fuel and its thermal power, while the power of the plasma reactor increases with the increase of the temperature. In contrast to the output power, this power increases as expected, even though the pyrolysis process ends at 1500 K. Therefore, it is obvious that a further increase of the process temperature above 1500 K does not make sense, since the additional energy would be spent on a further increase of the physical enthalpy of the products, formation of undesirable compounds, and dissociation of hydrogen. None of the above processes is desirable in the pyrolysis of natural gas. Increasing the physical enthalpy is not practical, considering that once the equilibrium concentration of the system is reached at the desired temperature, very rapid cooling, known as quenching, is required to prevent the reversibility of the process as well as the formation of undesirable compounds that would form during slow cooling. Considering that the heat dissipated during the quenching of the system represents a pure loss of the process, it is clear why a further increase in temperature is undesirable.

The energy at the input of the system is equal to the sum of useful energy and energy losses. The energy losses consist of the energy contained in the graphite byproduct, the energy extracted from the system by quenching, and other energy losses that are an order of magnitude less than the two mentioned. The efficiency of the process is shown in Fig. 5.

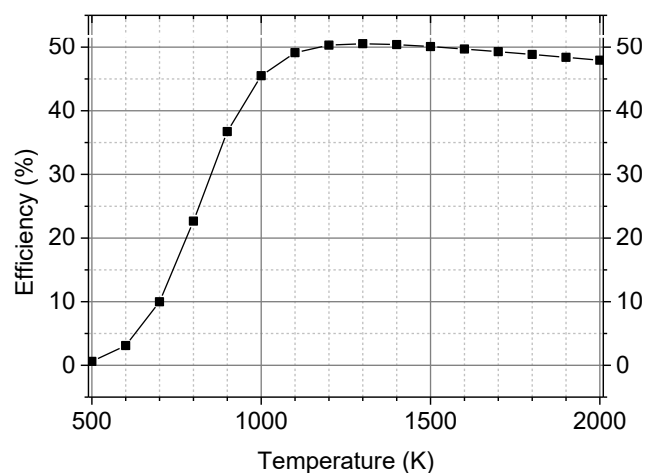


Fig. 6 The efficiency of the process

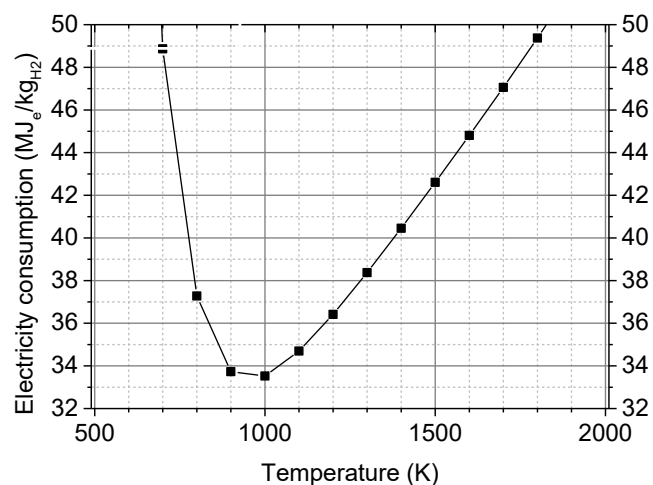


Fig. 7 Electricity consumption

From Fig. 6 it can be seen that the efficiency of the process increases with increasing temperature and reaches a maximum at a temperature of about 1200 K, which is about 50 %. However, as already analyzed, the process of pyrolysis of natural gas at this temperature is not yet complete, i.e., the proportion of hydrogen has not yet reached its maximum. In the temperature range of 1200-1500 K, the increase in the hydrogen content is about 1.3 % compared to the total value, and the increase in the power of the plasma reactor is about 17 %, which means that the energy of the plasma torch is mainly used to increase the physical enthalpy of the system. Considering that the increase of the physical enthalpy of the system is a pure loss and that the increase of the hydrogen content is negligible, it follows that the optimal temperature for the natural gas pyrolysis process is 1200 K, considering the energy analysis.

Fig. 7 shows the electricity consumption for hydrogen production, assuming that the degree of conversion to plasma energy is 100 %. From the figure it can be seen that about 36.5 MJ are needed to produce one kilogram of hydrogen at a temperature of 1200 K.

#### 4. CONCLUSION

The article deals with the process of pyrolysis of natural gas to obtain hydrogen in a low-temperature plasma reactor. The hydrogen yield was determined by calculating the equilibrium composition of the system using the Gibbs free energy minimization method. The applied methodology showed the temperature dependence of the equilibrium composition of the system. The results of the one-dimensional numerical analysis show that the efficiency of the process increases with increasing temperature and reaches its maximum at a temperature of 1200 K when an energy efficiency of about 50 % is achieved. The resulting system must be cooled (quenched) very quickly to prevent reversibility and the formation of undesirable compounds. In analyzing the process, it was assumed that the only useful product would be hydrogen, while carbon in the form of graphite was considered a byproduct. It

is certainly possible to use graphite in another form, but that could be the subject of new research in this area. Pyrolysis of natural gas produces undesirable and harmful compounds, mainly carbon monoxide, ammonia, hydrogen cyanide and nitrogen monoxide. The analysis of the obtained results has shown that from the ecological point of view, a lower process temperature is more advantageous. The developed model of the natural gas pyrolysis process in a low-temperature plasma reactor opens opportunities for further research aimed at the utilization of graphite by-products as well as the use of waste heat from the quenching process of the system. In addition, further analysis can be directed to the process of natural gas gasification in a low-temperature plasma reactor using water as the working medium.

## ACKNOWLEDGEMENT

This research was funded by the Ministry of Science, Technological Development and Innovation of the Republic of Serbia, Grant no. 451-03-47/2023-01/200017 («Vinča» Institute of Nuclear Sciences, National Institute of the Republic of Serbia, University of Belgrade)

## REFERENCES

- [1] \*\*, “The Renewable Energy Directive .” [https://energy.ec.europa.eu/topics/renewable-energy/renewable-energy-directive-targets-and-rules/renewable-energy-directive\\_en](https://energy.ec.europa.eu/topics/renewable-energy/renewable-energy-directive-targets-and-rules/renewable-energy-directive_en) (accessed Oct. 27, 2022).
- [2] A. Ajanovic, M. Sayer, and R. Haas, “The economics and the environmental benignity of different colors of hydrogen,” *Int J Hydrogen Energy*, vol. 47, no. 57, pp. 24136–24154, 2022, doi: 10.1016/j.ijhydene.2022.02.094.
- [3] International Energy Agency (IEA), “Global Hydrogen Review 2022,” 2022. [Online]. Available: [www.iea.org/t&c/](http://www.iea.org/t&c/)
- [4] S. Bepalko and J. Mizeraczyk, “Overview of the Hydrogen Production by Plasma-Driven Solution Electrolysis,” *Energies (Basel)*, vol. 15, no. 20, p. 7508, 2022, doi: 10.3390/en15207508.
- [5] M. Hrabovsky *et al.*, “Steam Plasma Methane Reforming for Hydrogen Production,” *Plasma Chemistry and Plasma Processing*, vol. 38, no. 4, pp. 743–758, 2018, doi: 10.1007/s11090-018-9891-5.
- [6] L. Barelli, G. Bidini, F. Gallorini, and S. Servili, “Hydrogen production through sorption-enhanced steam methane reforming and membrane technology: A review,” *Energy*, vol. 33, no. 4, pp. 554–570, 2008, doi: 10.1016/j.energy.2007.10.018.
- [7] D. H. Choi, S. M. Chun, S. H. Ma, and Y. C. Hong, “Production of hydrogen-rich syngas from methane reforming by steam microwave plasma,” *Journal of Industrial and Engineering Chemistry*, vol. 34, pp. 286–291, 2016, doi: 10.1016/j.jiec.2015.11.019.
- [8] H.-G. Park, S.-Y. Han, K.-W. Jun, Y. Woo, M.-J. Park, and S. K. Kim, “Bench-Scale Steam Reforming of Methane for Hydrogen Production,” *Catalysts*, vol. 9, no. 7, p. 615, 2019, doi: 10.3390/catal9070615.
- [9] E. Shagdar, B. G. Lougou, Y. Shuai, E. Ganbold, O. P. Chinonso, and H. Tan, “Process analysis of solar steam reforming of methane for producing low-carbon hydrogen,” *RSC Adv*, vol. 10, no. 21, pp. 12582–12597, 2020, doi: 10.1039/C9RA09835F.
- [10] K. S. Go, S. R. Son, S. D. Kim, K. S. Kang, and C. S. Park, “Hydrogen production from two-step steam methane reforming in a fluidized bed reactor,” *Int J Hydrogen Energy*, vol. 34, no. 3, pp. 1301–1309, 2009, doi: 10.1016/j.ijhydene.2008.11.062.

- 0338-14
- [11] S. Timmerberg, M. Kaltschmitt, and M. Finkbeiner, “Hydrogen and hydrogen-derived fuels through methane decomposition of natural gas – GHG emissions and costs,” *Energy Conversion and Management: X*, vol. 7, p. 100043, 2020, doi: 10.1016/j.ecmx.2020.100043.
  - [12] L. Weger, A. Abánades, and T. Butler, “Methane cracking as a bridge technology to the hydrogen economy,” *Int J Hydrogen Energy*, vol. 42, no. 1, pp. 720–731, 2017, doi: 10.1016/j.ijhydene.2016.11.029.
  - [13] H. F. Abbas and W. M. A. Wan Daud, “Hydrogen production by methane decomposition: A review,” *Int J Hydrogen Energy*, vol. 35, no. 3, pp. 1160–1190, 2010, doi: 10.1016/j.ijhydene.2009.11.036.
  - [14] M. Yousefi and S. Donne, “Technical challenges for developing thermal methane cracking in small or medium scales to produce pure hydrogen - A review,” *Int J Hydrogen Energy*, vol. 47, no. 2, pp. 699–727, 2022, doi: 10.1016/j.ijhydene.2021.10.100.
  - [15] J. X. Qian, T. W. Chen, L. R. Enakonda, D. bin Liu, J.-M. Basset, and L. Zhou, “Methane decomposition to pure hydrogen and carbon nano materials: State-of-the-art and future perspectives,” *Int J Hydrogen Energy*, vol. 45, no. 32, pp. 15721–15743, 2020, doi: 10.1016/j.ijhydene.2020.04.100.
  - [16] A. Iulianelli, S. Liguori, J. Wilcox, and A. Basile, “Advances on methane steam reforming to produce hydrogen through membrane reactors technology: A review,” *Catalysis Reviews*, vol. 58, no. 1, pp. 1–35, 2016, doi: 10.1080/01614940.2015.1099882.
  - [17] Z. Fan, W. Weng, J. Zhou, D. Gu, and W. Xiao, “Catalytic decomposition of methane to produce hydrogen: A review,” *Journal of Energy Chemistry*, vol. 58, pp. 415–430, 2021, doi: 10.1016/j.jechem.2020.10.049.
  - [18] L. Chen, Z. Qi, S. Zhang, J. Su, and G. A. Somorjai, “Catalytic Hydrogen Production from Methane: A Review on Recent Progress and Prospect,” *Catalysts*, vol. 10, no. 8, p. 858, 2020, doi: 10.3390/catal10080858.
  - [19] P. Stefanović, P. Pavlović, Ž. Kostić, and D. Cvetinović, “Plazma proces proizvodnje čađi i vodonika iz metana,” in *GAS '97*, 1997, pp. 340–348.
  - [20] L. Bromberg, D. R. Cohn, A. Rabinovich, and N. Alexeev, “Plasma catalytic reforming of methane.”
  - [21] F. Saleem, J. Harris, K. Zhang, and A. Harvey, “Non-thermal plasma as a promising route for the removal of tar from the product gas of biomass gasification – A critical review,” *Chemical Engineering Journal*, vol. 382, no. June 2019, p. 122761, 2020, doi: 10.1016/j.cej.2019.122761.
  - [22] A. H. Khoja *et al.*, “Hydrogen Production from Methane Cracking in Dielectric Barrier Discharge Catalytic Plasma Reactor Using a Nanocatalyst,” *Energies (Basel)*, vol. 13, no. 22, p. 5921, 2020, doi: 10.3390/en13225921.
  - [23] C. S. Kalra, A. F. Gutsol, and A. A. Fridman, “Gliding arc discharges as a source of intermediate plasma for methane partial oxidation,” *IEEE Transactions on Plasma Science*, vol. 33, no. 1, pp. 32–41, Feb. 2005, doi: 10.1109/TPS.2004.842321.
  - [24] X. Guofeng and D. Xinwei, “Optimization geometries of a vortex gliding-arc reactor for partial oxidation of methane,” *Energy*, vol. 47, no. 1, pp. 333–339, Nov. 2012, doi: 10.1016/j.energy.2012.09.032.
  - [25] M. Gautier, V. Rohani, and L. Fulcheri, “Direct decarbonization of methane by thermal plasma for the production of hydrogen and high value-added carbon black,” *Int J Hydrogen Energy*, vol. 42, no. 47, pp. 28140–28156, 2017, doi: 10.1016/j.ijhydene.2017.09.021.
  - [26] A. E. E. Putra, S. Nomura, S. Mukasa, and H. Toyota, “Hydrogen production by radio frequency plasma stimulation in methane hydrate at atmospheric pressure,” *Int J Hydrogen Energy*, vol. 37, no. 21, pp. 16000–16005, 2012, doi: 10.1016/j.ijhydene.2012.07.099.
  - [27] O. Akande and B. Lee, “Plasma steam methane reforming (PSMR) using a microwave torch for commercial-scale distributed hydrogen production,” *Int J Hydrogen Energy*, vol. 47, no. 5, pp. 2874–2884, 2022, doi: 10.1016/j.ijhydene.2021.10.258.

- 0338-15
- [28] D. Czyilkowski, B. Hrycak, M. Jasiński, M. Dors, and J. Mizeraczyk, “Microwave plasma-based method of hydrogen production via combined steam reforming of methane,” *Energy*, vol. 113, pp. 653–661, 2016, doi: 10.1016/j.energy.2016.07.088.
- [29] Q. Wang, J. Wang, T. Zhu, X. Zhu, and B. Sun, “Characteristics of methane wet reforming driven by microwave plasma in liquid phase for hydrogen production,” *Int J Hydrogen Energy*, vol. 46, no. 69, pp. 34105–34115, 2021, doi: 10.1016/j.ijhydene.2021.08.006.
- [30] M. M. Moshrefi, F. Rashidi, H. R. Bozorgzadeh, and S. M. Zekordi, “Methane Conversion to Hydrogen and Carbon Black by DC-Spark Discharge,” *Plasma Chemistry and Plasma Processing*, vol. 32, no. 6, pp. 1157–1168, 2012, doi: 10.1007/s11090-012-9408-6.
- [31] X. Tu and J. C. Whitehead, “Plasma dry reforming of methane in an atmospheric pressure AC gliding arc discharge: Co-generation of syngas and carbon nanomaterials,” *Int J Hydrogen Energy*, vol. 39, no. 18, pp. 9658–9669, 2014, doi: 10.1016/j.ijhydene.2014.04.073.
- [32] Keun Su Kim, Jun Ho Seo, Jun Seok Nam, Won Tae Ju, and Sang Hee Hong, “Production of hydrogen and carbon black by methane decomposition using DC-RF hybrid thermal plasmas,” *IEEE Transactions on Plasma Science*, vol. 33, no. 2, pp. 813–823, 2005, doi: 10.1109/TPS.2005.844526.
- [33] A. Abánades, C. Rubbia, and D. Salmieri, “Thermal cracking of methane into Hydrogen for a CO<sub>2</sub>-free utilization of natural gas,” *Int J Hydrogen Energy*, vol. 38, no. 20, pp. 8491–8496, 2013, doi: 10.1016/j.ijhydene.2012.08.138.
- [34] <https://www.spglobal.com/commodityinsights/en/ci/products/hydrogen-carbon-black-methane-pyrolysis.html>, assessed 28.04.2022
- [35] D. Cvetinović, A. Erić, P. Škobalj, N. Milutinović, and V. Bakić, “Thermodynamic Modeling as a Tool for Design and Optimisation of Thermal Plasma Reactor for PCBs Decomposition,” in *5th Conference on Sustainable Development of Energy, Water and Environment Systems*, 2022, p. 224.
- [36] D. Cvetinović, A. Erić, N. Milutinović, P. Škobalj, and V. Bakić, “Thermodynamic Analysis of the Process of Decomposition of Hazardous Waste in Thermal Plasma with the use of Different Working Media,” in *16th Conference on Sustainable Development of Energy, Water and Environment Systems*, 2021, p. 726.
- [37] A. Erić, D. Cvetinović, N. Milutinović, P. Škobalj, and V. Bakić, “Combined parametric modelling of biomass devolatilisation process,” *Renew Energy*, vol. 193, pp. 13–22, Jun. 2022, doi: 10.1016/j.renene.2022.04.129.
- [38] G. V. Belov, V. S. Iorish, and V. S. Yungman, “IVTANTHERMO for Windows - database on thermodynamic properties and related software,” *CALPHAD*, vol. 23, no. 2, pp. 173–180, 1999, doi: 10.1016/S0364-5916(99)00023-1.
- [39] Belov G.V., Dyachkov S.A., Levashov P.R., et al. The IVTANTHERMO --- online database for thermodynamic properties of individual substances with web interface. *J. Phys.: Conf. Ser.*, 2018, vol. 946, art. 012120. DOI: <https://doi.org/10.1088/1742-6596/946/1/012120>
- [40] Gurvich, L.V.: Reference books and data banks on the thermodynamic properties of individual substances. *Pure Appl. Chem.* 61, 1027–1031 (1989).
- [41] Belov, G.V., Dyachkov, S.A., Levashov, P.R., Lomonosov, I.V., Minakov, D.V., Morozov, I.V., Sineva, M.A., and Smirnov, V.N.: The IVTANTHERMO-Online database for thermodynamic properties of individual substances with web interface. *J. Phys. Conf. Ser.* 946, 012120 (2018).